Application of Simulation Code, GEOTH3D, on the Ogachi HDR Site

Takeshi Yamamoto', Kouichi Kitano', Yasuhiro Fujimitsu[2], and Hiroshi Ohnishi[3]
'Central Research Institute of Electric Power Industry, Abiko Laboratory,
1646 Abiko, Abiko City, Chiba, 270-11, Japan
[2]Kyushu University, Hakozaki 6-10-1, Higashi-ku, Fukuoka, 812-81, Japan
[3]Denryoku Computing Center, Abiko Center, 1646 Abiko, Abiko City, Chiba, 270-11, Japan

ABSTRACT

A mathematical model composed of two equations for mass and energy balance based on Darcy's law is suitable for numerical simulation of thermal hydraulic behavior in geothermal and Hot Dry Rock reservoirs. The model may describe the three-dimensional behavior of both water and heat transport in porous media. The simulating code for HDR, named "GEOTH3D," [Yamamoto et al., 1995] was developed at the Central Research Institute of Electric Power Industry (CRIEPI), and consisted of numerical methods based on three-dimensional finite difference approximations with fully implicit Newton-Raphson treatment of nonlinear terms. The three-dimensional physical properties of the modeled reservoir were determined by combining the data of Acoustic Emissions with the data of permeability tests. We can estimate the continuous temperature and pressure changes in the modeled reservoir and the recovery flow rate. In this paper, we treat the recovery prediction method with comparison to the field data that obtained at Ogachi HDR site in 1994 and 1995 [Yamamoto et al., 1996].

INTRODUCTION

At the Ogachi Hot Dry Rock experiment site, there are two boreholes drilled through an artificial reservoir. In 1991, we formed fractures in the lower part of the reservoir by injecting 10,000 tons of water into the open-hole zone in the bottom-hole part of the injection well at from 990 to 1,000m depth. In the next year, 1992, we formed the upper part of the reservoir by injecting *5,000* tons of water into the open-hole section at 711 - 719m. The second well was drilled as a production well, to penetrate the fractures [Kaieda et al., 19931.

We conducted hydraulic circulation tests for 20 days in 1993, 151 days in 1994, and 30 days in 1995. Before the 151-day circulation test, in 1994, we operated a reservoir stimulation by injecting 3,100 tons of water into the production well. Before the 30-day circulation in 1995, we made an additional drilling and a reservoir stimulation at the injection wellbore to gain the injecting section for 27m, then we also operated the second reservoir stimulation at the production well. The hydraulic recoveries were about 10% and 30% in 1994 and 1995, respectively.

MATHEMATICAL MODEL IN THREE-DIMENSIONAL EQUATIONS

Mass and Momentum Balance

$$\frac{\partial m}{\partial t} - \sum_{\alpha=1}^{2} \mathrm{div}\left\{\left(\frac{\rho}{\mu}k\right)_\alpha \mathbf{K}\cdot \mathrm{grad}p - \left(\frac{\rho^2}{\mu}k\right)_\alpha \mathbf{K}\cdot\mathbf{g}\right\} = q_m \qquad (1)$$

where

$$m = \phi\rho = \phi\sum_{\alpha=1}^{2}(S_\alpha\rho_\alpha),\ \sum_{\alpha=1}^{2} S_\alpha = 1 \qquad (2)$$

$$\phi = \phi_0 + \beta_r(p - p_0) \qquad (3)$$

$$q_m = \sum_{\alpha=1}^{2} q_{m\alpha} = q_{mw} + q_{ms} \qquad (4)$$

The mass balance for water for both single and two phase conditions, under the assumption of Darcy's law for multiphase flow, may be described as follows:

In equation (1), α=1 and a=2 mean water phase and steam phase, respectively, ϕ is the porosity, ϕ_0 is the initial porosity, β_r is the compressibility coefficient of the rock, p is piezometric pressure, p_0 is initial phase pressure. S is the volumetric saturation rate, ρ is the water density, k is the relative permeability of the porous medium, m is the total mass of the fluid, t is the

ıme, **K** is the intrinsic permeability tensor of the orous medium, μ is the dynamic viscosity, q_m is the ource term, and **g** is the gravitational constant vector.

Snergy Balance

$$= -\sum_{\alpha=1}^{2} \mathrm{div}\left\{\left(\frac{\rho}{\mu}\mathrm{kh}\right)_\alpha \mathbf{K}\cdot\mathrm{gradp} - \left(\frac{\rho^2}{\mu}\mathrm{kh}\right)_\alpha \mathbf{K}\cdot\mathbf{g}\right\}$$

$$div\left\{K_m\left(\frac{\partial T}{\partial p}\right)_h \mathrm{gradp} + K_m\left(\frac{\partial T}{\partial h}\right)_p \mathrm{gradh}\right\} = q_e \qquad (5)$$

here

$$= mh + (1-\phi)\rho_r h_r = \phi\rho h + (1-\phi)\rho_r c_r T$$

$$= \phi\sum_{\alpha=1}^{2}(S_\alpha\rho_\alpha h_\alpha) + (1-\phi)\rho_r c_r T \qquad (6)$$

$$= q_m h = \sum_{\alpha=1}^{2} q_{m\alpha} h_\alpha = q_{mw} h_w + q_{ms} h_s \qquad (7)$$

$$= \frac{\sum_{\alpha=1}^{2}(S_\alpha\rho_\alpha h_\alpha)}{\sum_{\alpha=1}^{2}(S_\alpha\rho_\alpha)} = \frac{(S_w\rho_w h_w + S_s\rho_s h_s)}{\rho} \qquad (8)$$

A simplified energy balance for water, steam, and rock nay be written as follows:

Where, r means rock, K_m is the dispersion coefficient or heat conduction in the porous medium, h is the enthalpy of the water-steam mixture. h_w and h_s are the specific enthalpies of water and steam, respectively. c_r s the specific heat of the rock, and T is temperature.

*Constitutive **Relationships***

The simplified balance equations (1) and ***(5)*** are based on the following assumptions [Faust et al., 19791:

1) Capillary pressure effects are neglected.
2) Water, steam, and rock are thermally equilibrated.
3) The reservoir water is either single phase or two phases.
4) Relative permeability is a function of only liquid volume saturation rate; hysteresis is neglected.
5) Viscosities are considered as functions of pressure and temperature.
6) Porosity is a linear function of pressure, as shown in (3).
7) Rock density, reservoir thickness, and intrinsic permeability tensor are arbitrarily given in three dimensional space.
8) The mass and energy source terms q_m and q_e, respectively, represent the amount of mass and enthalpy due to source-sink capacity. In a two-phase region, the source-sink term of mass and energy is defined as $q_m = q_{mw} + q_{ms}$ and $q_e = q_{ew} + q_{es}$, respectively, as defined in (4) and (7).
9) Rock enthalpy is a linear function of temperature, $h_r = c_r T$, as given in ***(6)***.

Recoverly flow rate prediction

A brief summary of the calculation **is** as follows :

The total incoming flow rate at numerical time step "t" in the production point is set to be treated as a production flow rate and to disappear at the next time step "t+Δt". There is no vacuum at the production points to maintain production flow rate.

OGACHI RESERVOIR MODEL

Finite-Difference Blocks

The three-dimensional conceptual raservoir model of the Ogachi site is divided into finite-difference blocks. The blocks are distributed around the wells in a cube. A segmental length of the minimum cube is 10m. Fig.1 shows central area of finite-difference blocks used for this simulation.

Application of AE Data

Seismic center and magnitude of micro-earthquakes (Acoustic Emission, AE) can be determined from field monitoring data. We made some treatment to the field data of AE and translated the treated values into permeability values by making two assumptions as follows:

[1]Hydraulic flow in the fractured **rack** can be represented by the flow through a porous media.
[2] Mean permeability values at the specific areas are proportionate to magnitude values of AE.

We applied a three-dimensional averaging method in treating the **AE** data, then made three-dimensional permeability maps as shown in Fig.2 - Fig.5. The data of AE [Kaieda et al., 1995] are treated in cubes with 20m of segmental length. After this treatment, the blocks distributed around the wells are divided into cubes with 10m segmental length. The summed and averaged values are named cumulative magnitudes, $C.M_B$. The way of treating AE data is shown in the following list:

1) Translating magnitude, M_B, into energy, E_S, by applying Gutenberg-Richter'smodel for body wave.

$$\log E_S = 5.8 + 2.4 M_B$$

2)Summing up all energy of AE events occurred in each 20m segmental length of cube area. We assumed the cumulative energy concentrated at the center of each block.

3) Picking up eighteen blocks bordering on six surfaces and twelve segments in each core block, then making weighted averaging among eighteen bordering blocks and the core block. Distance between the center of core block and that of the bordering block is set as "r". We assumed the seismic area as smaller than the 20 (segmental length) times the square root of *2* meters.

$$r < 20\sqrt{2} \quad (m)$$

We obtain the averaged value of energy, "$E_{i,j,k}$", Owith applying weighted parameter "w_l". This weighted averaging method is usually used at image processing.

$$E_{i,j,k} = \sum_{l=0}^{18} w_l E_l$$

$$w_l = \frac{\frac{1}{r_l^2}}{\sum_{i=0}^{18} \frac{1}{r_l^2}} \quad , \quad \frac{1}{r_0} = 1$$

4) Applying Laplacian Filtering method to the three-dimensional map of E_{ijk}.

5) Translating E_{ijk} to cumulative magnitude, $C.M_B$, by applying Gutenberg-Richter'smodel. The $C.M_B$ value ranged from -4 to -0.1.

6) Translating the cumulative magnitude into permeability by making a combination relationship with the results of hydraulic communication tests. The method is shown in the following section.

Application of permeability data

In modeling a reservoir of Ogachi site, we used the field data of AE combining the results of hydraulic permeability tests that operated at each injection and production well. The reservoir was formed in 1991 and 1992, then hydraulic circulation tests were operated for 20 days in 1993, 151 days in 1994, and 30 days in 1995. Prior to the last two circulating periods, hydrauric stimulations to the production wellbore were operated, and the. The stimulating method was to inject highly pressurized water into the well for short terms, aiming to stimulatejust around the well. AE was monitored during each of those operations, from 1991 to 1995. The communication tests were operated in each year, at both the beginning and the end of the hydraulic circulation tests.

The initial permeability of the site measured at the injection well just before the first hydraulic stimulation in 1991, and the result of hydraulic communication test operated just before the last hydraulic circulation are shown in the below.

	1991	1995
permeability (m')	1×10^{-16}	3×10^{-15}

The ***in site*** permeability in 1991 shows an evaluation value for virginal rock. We set this value, 1×10^{-16} (m^2), as the lowest permeability block distribution used for the numerical simulation. The other evaluation value measured in 1995 shows the mean hydraulic permeability between the injection and production wells after some stimulations to those wells. We set a somewhat higher value, 1×10^{-14}(m^2), as the highest value in the permeability distribution blocks.

Combination of jield datu

Both values of $C.M_B$, ranged from -4 to -0.1, and permeability, ranged from 1×10^{-16} to 1×10^{-14} (m^2), were divided into five steps. The initial rock porosity was ranged from 0.004 to 0.04 in 1991. We assumed the porosity of matrix ranges from 0.001 to 0.1. The porosity value was also divided into five steps as shown below. The combination relationship among $C.M_B$, permeability (P), and matrix porosity (ϕ) is shown in Fig.2. We assumed a linear relationship among those values as folows:

$C.M_B$:	-4- -3.7	-3.7- -2.8	-2.8- -1.9	-1.9- -1	-1- -0.1
$P(m^2)$:	1×10^{-16}	5×10^{-16}	2×10^{-15}	5×10^{-15}	1×10^{-14}
ϕ :	0.001	0.005	0.02	0.05	0.1

Modeled reservoir

Three-dimensionalmodeled reservoir of Ogachi site is divided into finite-differenceblocks. The blocks consisted of cubes with 10m segmental length, and rectangular solids with variable segmental lengths. The calculation domain is the same as that of the last simulation, 1,920m (W-E) x 1,860m **(S-N)** x 725m (thickness). The number of finite-differenceblocks is 32 (W-E) x 32 **(S-N)** x 24 (thickness), totaling 24,576 of blocks in the calculation domain. Fig.3 and Fig.4

show horizontal plain views of permeability distribution in 1994 modeled reservoir at 1000m and 1150m depth, respectively. Fig.5 and Fig.6 show the plain views of 1995 modeled reservoir at 1000m and 1150m depth, respectively. The ordered (0, 0, 0) represents the position of injection well head. The permeability condition, especially around the wells, was much improved by the last wellbore stimulation that operated in 1995.

RECOVERY FLOW RATE SIMULATION

In this paper, we specifically treat recovery flow rate simulation. Fig.7 shows the actual data during the 30-day hydraulic circulation test in 1995. The hydraulic recovery flow rate was 22% on the 25th day and 31% on the 30th day. The wellhead pressure at the production well was lowered slightly during the last two days to evaluate the relation between the wellhead pressure and the flow rate.

Outflow points in the production well

In 1995, outflows at specific production points in the well weren't detected, so we couldn't determine the depths of individual production points and their outflow rates. Fig.8 shows temperature changes in the production well. The profile of September 21st showes two major thermal depressed points at around 750m and 1080m well-along depth. These points seemed to allow a large amount of hydraulic intrusion during the stimulation period. There should be a strong connection between the wellbore and the fractures. The 29th day profile shows a slight temperature profile change at 730m depth. This phenomenon indicates an outflow point at that depth in the well. In 1994, an outflow point was also detected at the same position by the spinner measurement [Yamamotoet al., 19951. For those reasons, we set production points locating at 730m and 1080m well-along depth, 730m and 1060m vertical depth, respectively.

Injection points and flow rates in the injection well

The injection rates at the two points in the injection well weren't detected either. We use here the same condition that was used in the first paper. Fig.9 shows the inclinations of the wells, positions of injection and production points, and the injection ratio of the injection points.

A specified injection flow rate profiles that used in the numerical simulation is shown in Fig. 10, flowing at the constant rate as 27th. The injection flow rate was divided into ratio of 30% and 70%, at upper and lower injecting points respectively. We made two analyses by applying two modeled reservoirs, typed as 1994 and 1995 in Fig.3-Fig.6.

RESULTS

Profiles of predicted recovery flaw rates at the 27t/h injection rate are shown in Fig. 10. In this analysis, we couldn't apply optional pressures to the production points, due to the numerical treatment in the code. From this reason, the analyzed racovery values should be somewhat greater than the field data. We need some revision in the code to clear this problem.

Applying 1994 modeled reservoir

The hydraulic circulating conditions at the field in 1994 were as follows:

Injection rate	30t/h	45th
Injection wellhead pressure	12Mpa	16Mpa
Production rate	2.6t/h	3.7t/h
Production wellhead pressure	0.5Mpa	0.6Mpa
Temperature at wellhead	150C.d	155C.d.

The actual hydraulic recoveries in 1994 were about 10% with applying production wellhead pressure. The result of the simulation applying 11994modeled reservoir is as follows:

Injection rate	27t/h
Production rate at 730m depth	2.54t/h
Production rate at 1,060m depth	5.65t/h
Recovery	30.3%

Applying 1995 modeled reservoir

Actual circulating conditions at the field in 1995 were as follows:

Injection rate	30t/h
Injection wellhead pressure	6.3Mpa
Production rate	9t/h
Production wellhead pressure	0.8Mpa
Temperature at wellhead	160C.d

The actual hydraulic recovery in 1995 was about 30%, 3 times higher than that in 1994. The gain in the recovery was caused by the wellbore stimulations. The

result of the simulation applying 1995 modeled reservoir is as follows:

Injection rate	27t/h
Production rate at 730m depth	1.72t/h
Production rate at 1,060m depth	10.4t/h
Recovery	44.9%

The analyzed total recovery was 44.9%, about 1.5 times higher than the case of applying 1994 modeled reservoir. We can say that the simulated value agrees fairly well with the actual value. We could simulate the effect of wellbore stimulations by using our reservoir modeling method. Fig.3-Fig.6 show the improvement of permeability especially around the wellbores.

In this study, we couldn't compare the simulated and actual pressure values at each production and injection points with in the wellbores because we didn't measure the pressure distribution in the wells. Comparison of pressure distributions may be necessary to evaluate the reliability of this simulation technique. Further study of this simulation technique will be made in the future.

ACKNOWLEDGMENTS

Thanks to Dr. Yoshinao Hori and Dr. Hideshi Kaieda (belonging to CRIEPI) for offering the field data and giving us much advice on treating the data. Also to Dr. Nobukazu Tanaka, Dr. Yuzuru Eguchi and Takashi Nishihara (belonging to CRIEPI) for giving us much technical advice in cording GEOTH3D.

REFERENCES

Yamamoto, T., Fujimitsu, Y., Ohnishi, H., 1995. "Hot Dry Rock Reservoir 3D Simulation of the Ogachi Site", Geothermal Resources Council Transactions, Vol. 19, PP. 287-294

Yamamoto, T., Kitano, K., Tanaka, N., Ohnishi, H., 1996. "Hot Dry Rock Reservoir 3D Simulation of the Ogachi Site II", Geothermal Resources Council Transactions, Vol. 20, PP. 467-474

Kaieda, H., Kiho, K., and Motojima, I., 1993, Multiple Fracture Creation for Hot Dry Rock Development : Trends in Geophysical Research Vol. 2, pp. 127-139.

Faust, C.R., and Mercer, J.W., 1979, "Geothermal Reservoir Simulation 1. Mathematical Models for Liquid- and Vapor- Dominated Hydrothermal Systems", Water Resources Research Vol. 15, no. 1, pp. 23-30.

Kaieda, H., Fujimitsu, **Y.**, Yamamoto, T., Mizunaga, H., Ushijima, K., and Sasaki, **S.,** 1995, "AE and Mise-a-la-masse Measurements During a 22-day Water Circulation Test at The Ogachi HDR Site", World Geothermal Congress Transaction Vol.4, pp. 2695-2700.

Faust, C.R., and Mercer, J.W., 1979, "Geothermal Reservoir Simulation 2. Numerical Solution Techniques for Liquid- and Vapor- Dominated Hydrothermal Systems", Water Resources Research Vol. 15, no. 1, pp. 31-46.

Mercer, J.W., and Faust, C.R., 1979, "Geothermal Reservoir Simulation 3. Application of Liquid- and Vapor- Dominated Hydrothermal Modeling Techniques to Wairakei, New Zealand", Water Resources Research Vol. 15, no. 3, pp. 653-671.

Gringarten, A. C., Witherspoon, P. **A.,** and Ohnishi, **Y.,** 1975, "Theory of Heat Extraction Hot Dry Rock', Journal of Geophysical Research Vol. 80, No. 8.

Utsu, T., 1977, Seismology : Kyouritsu Shyuppan Publisher, pp. 126-129 (in Japanese)

Utsu, T., 1987, Encyclopedia of Earthquake : sakura Shyoten Publisher, pp. 49-57 (in Japanese)

Sahimi, M., 1995, Flow and Transport in Porous Media and Fractured Rock : VCH Verlagsgesellschaft mbH, Weinheim

Armstead, H. C. H., and Tester, J. **W.,** 1987, Heat Mining : E. & F. N. Spon Ltd

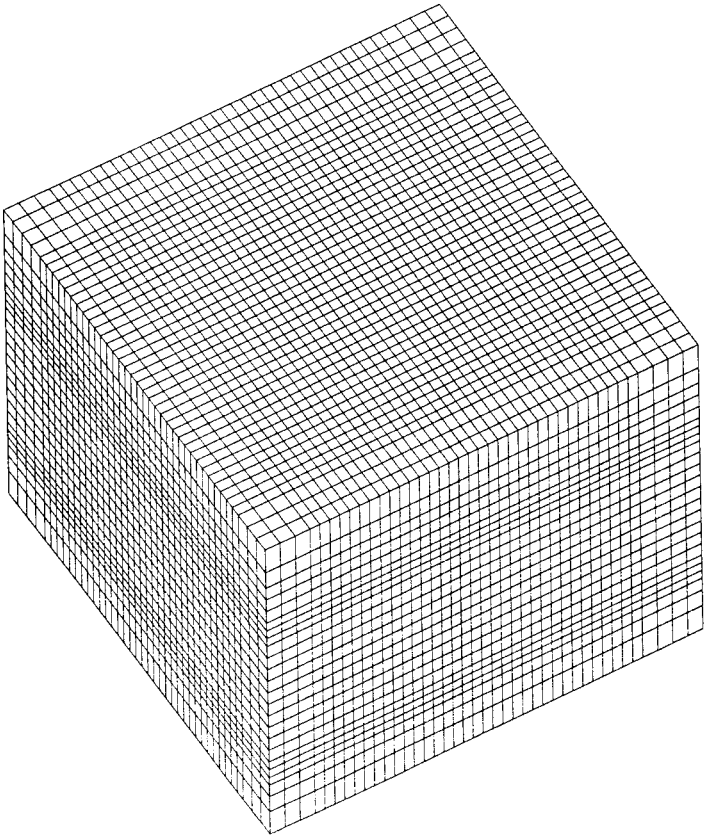

Fig.1 Central area of finite-difference blocks

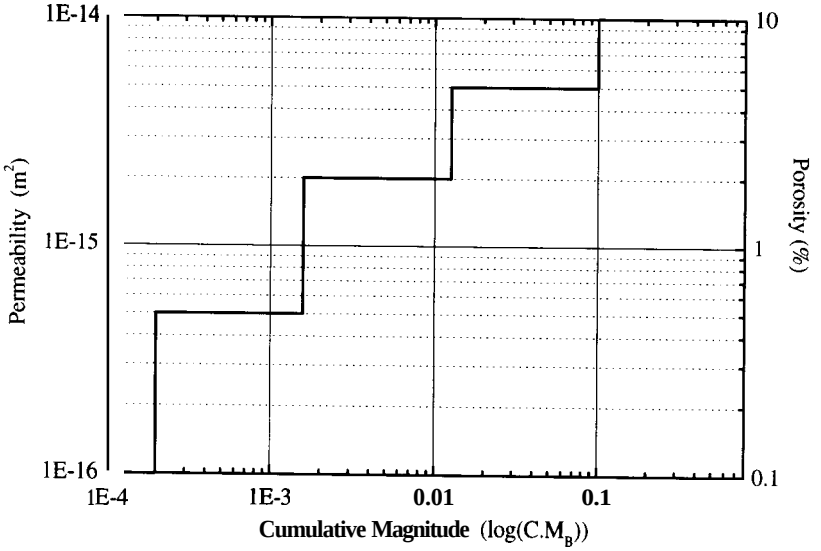

Fig.2 **Relationships between C.M_B, P, and Φ**

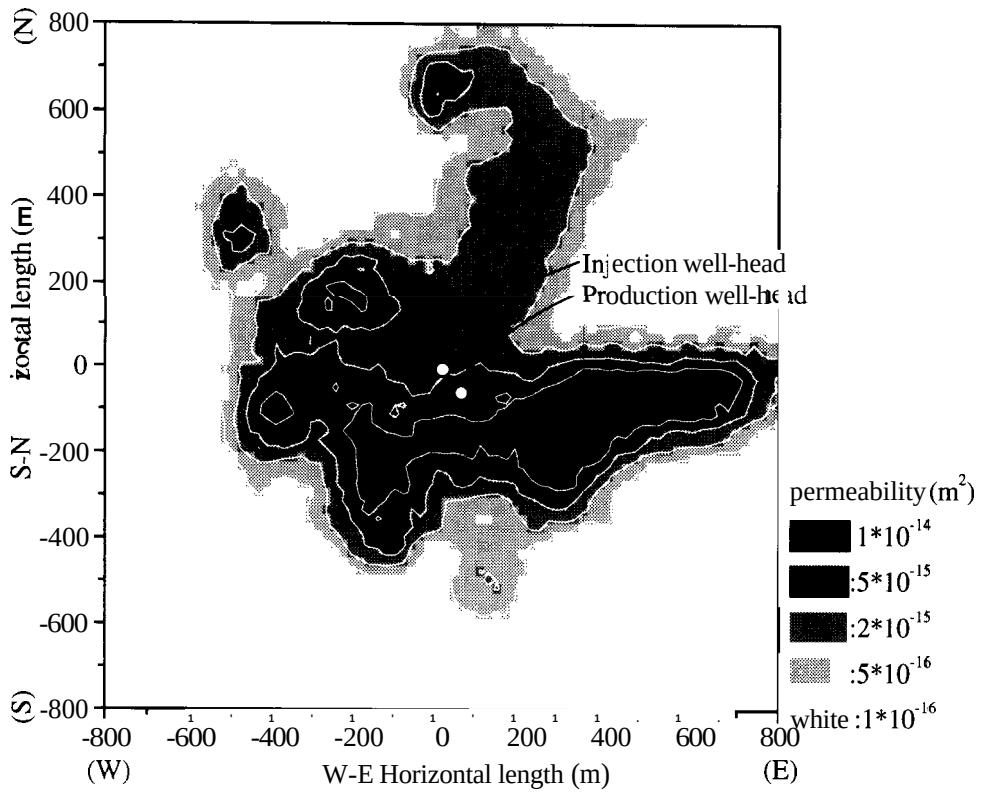

Fig.3 Horizontal permeability distribution, 1000m depth, in 1994

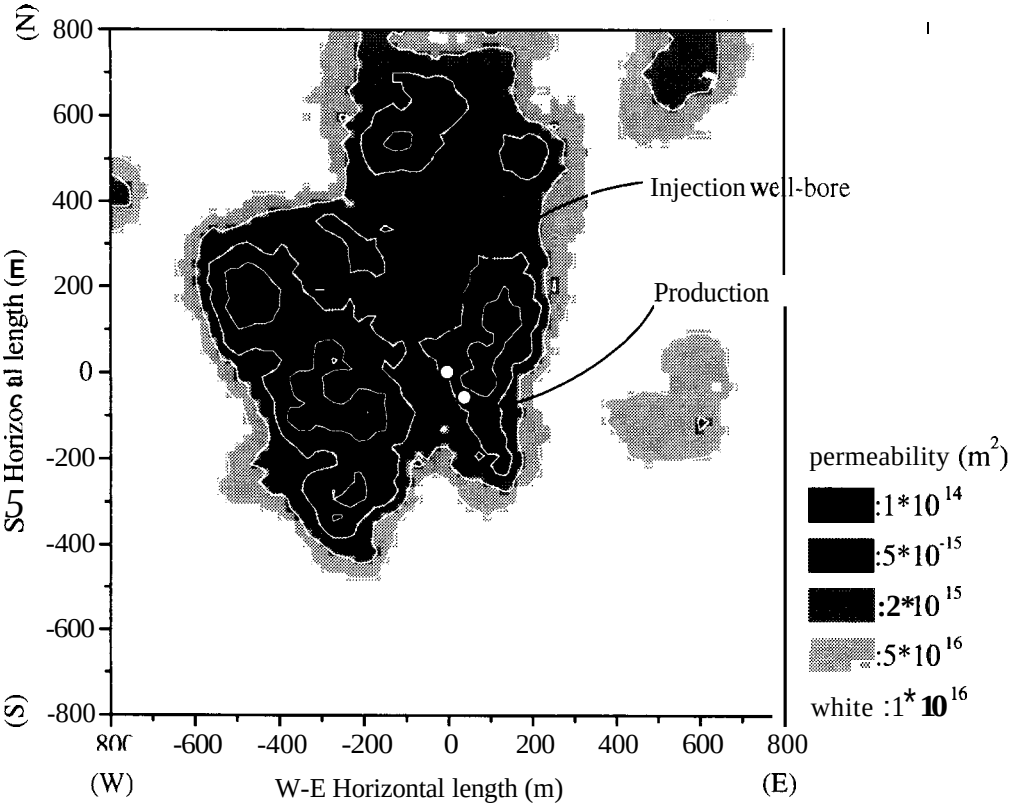

Fig.4 Horizontal permeability distribution, 1150m depth, in 1994

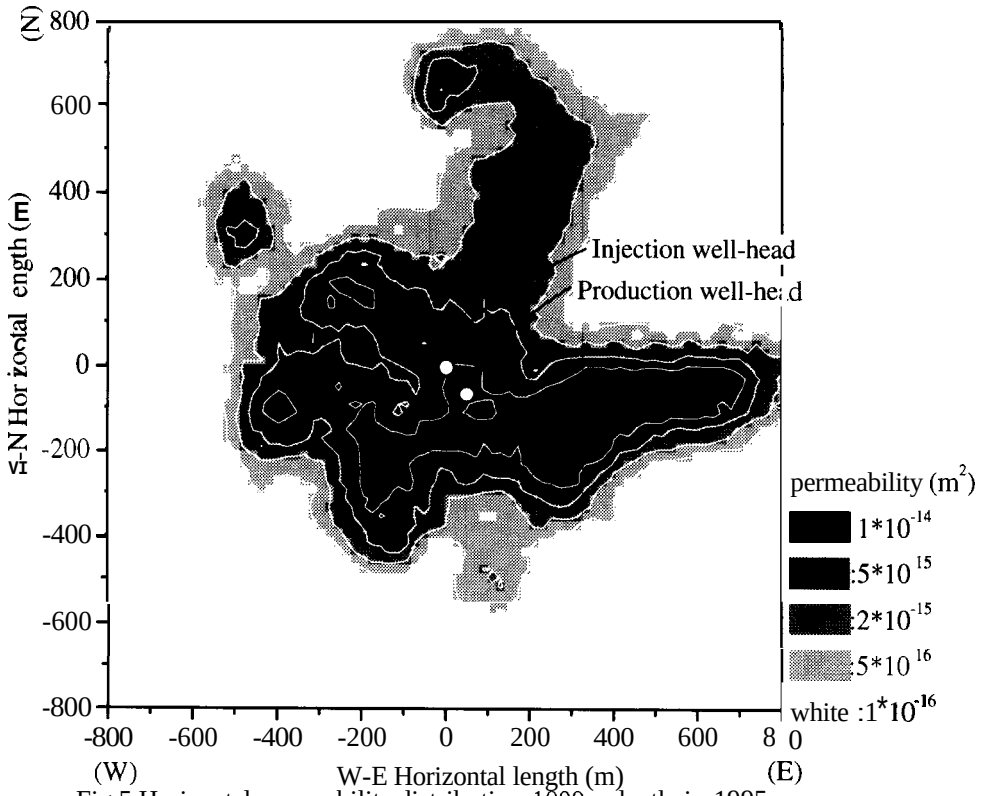

Fig.5 Horizontal permeability distribution, 1000m depth, in 1995

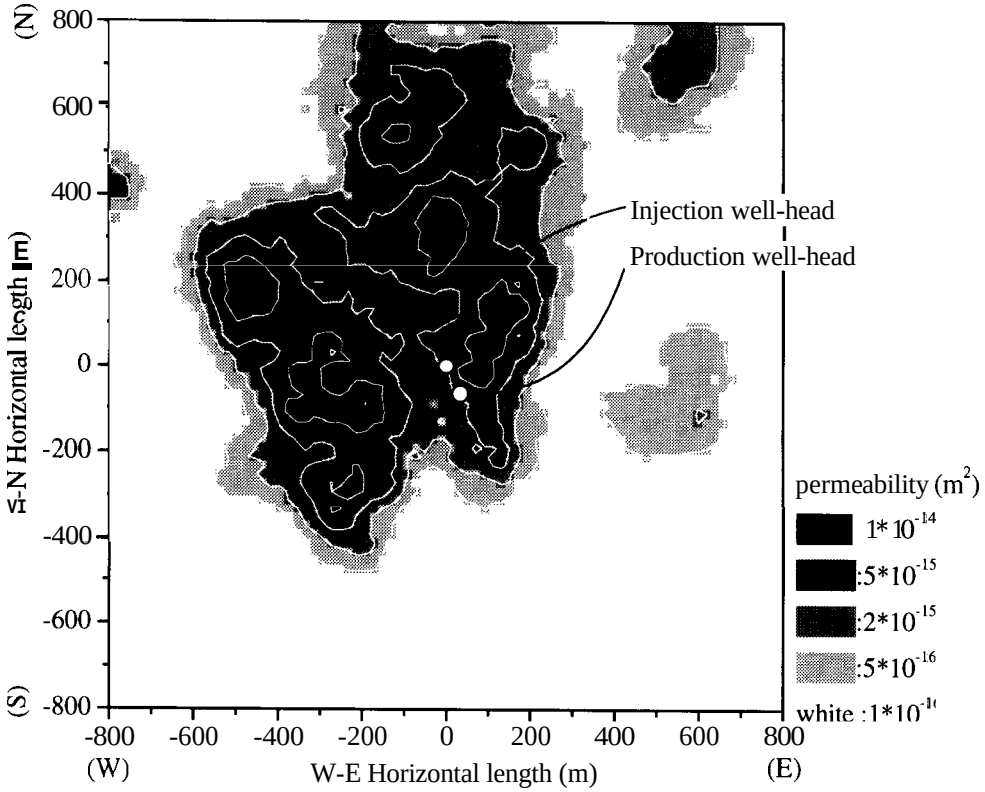

Fig.6 Horizontal permeability distribution, 1150m depth, in 1995

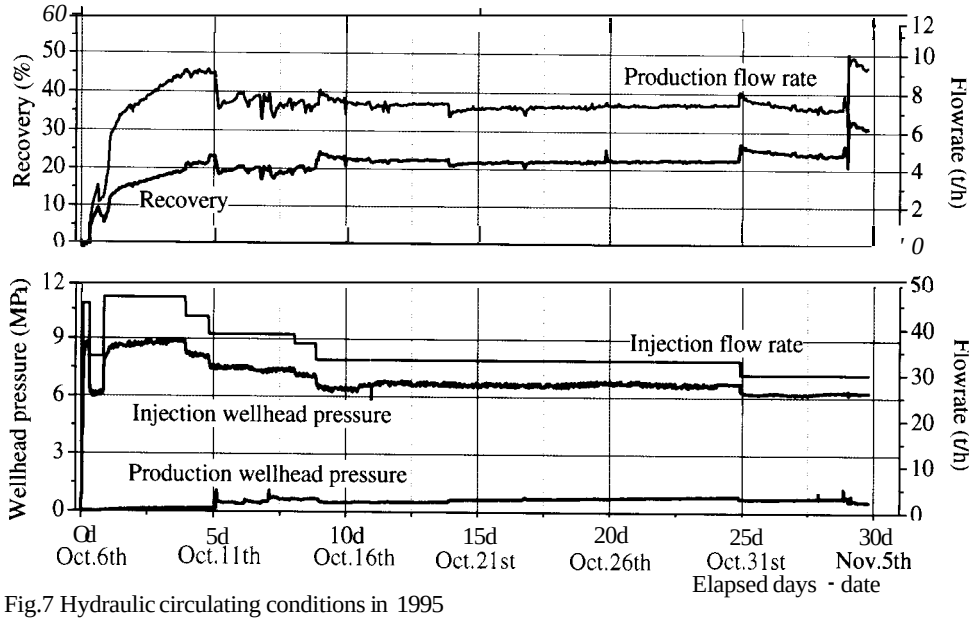

Fig.7 Hydraulic circulating conditions in 1995

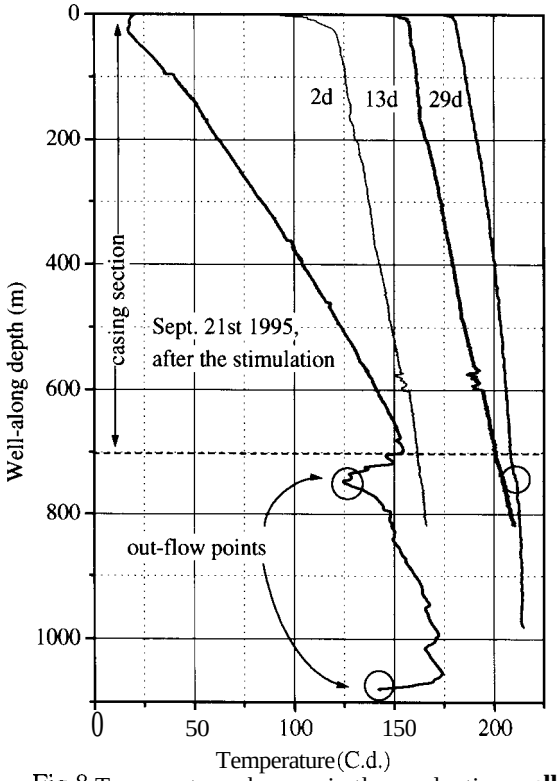

Fig.8 Temperature changes in the production **well** in 1995

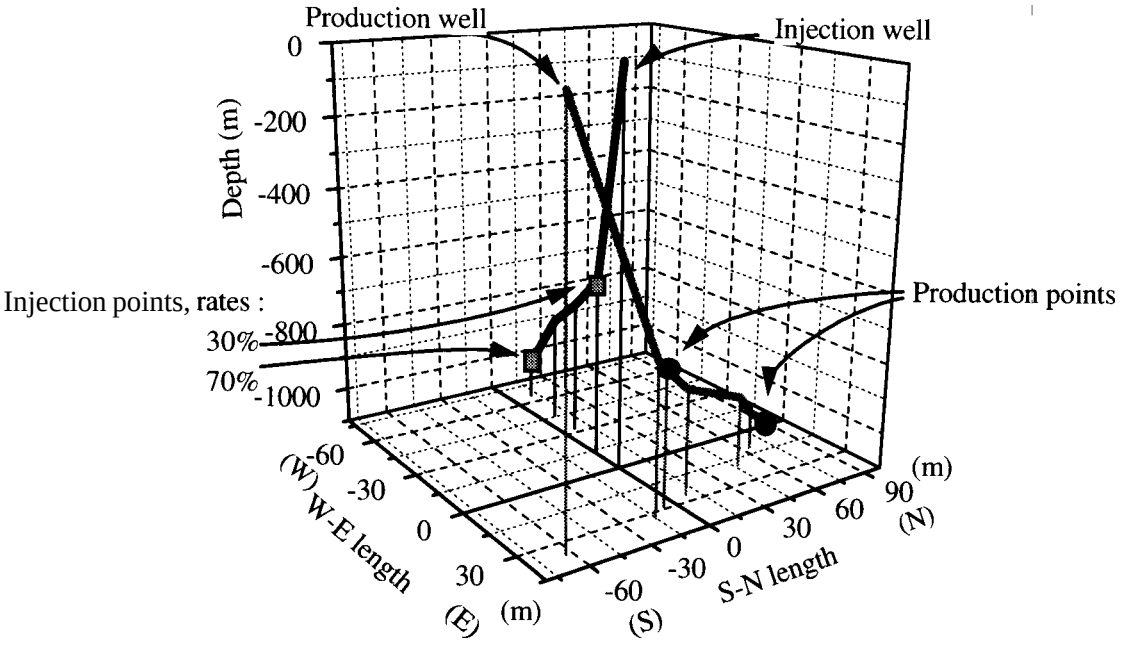

Fig.9 Injection and production points

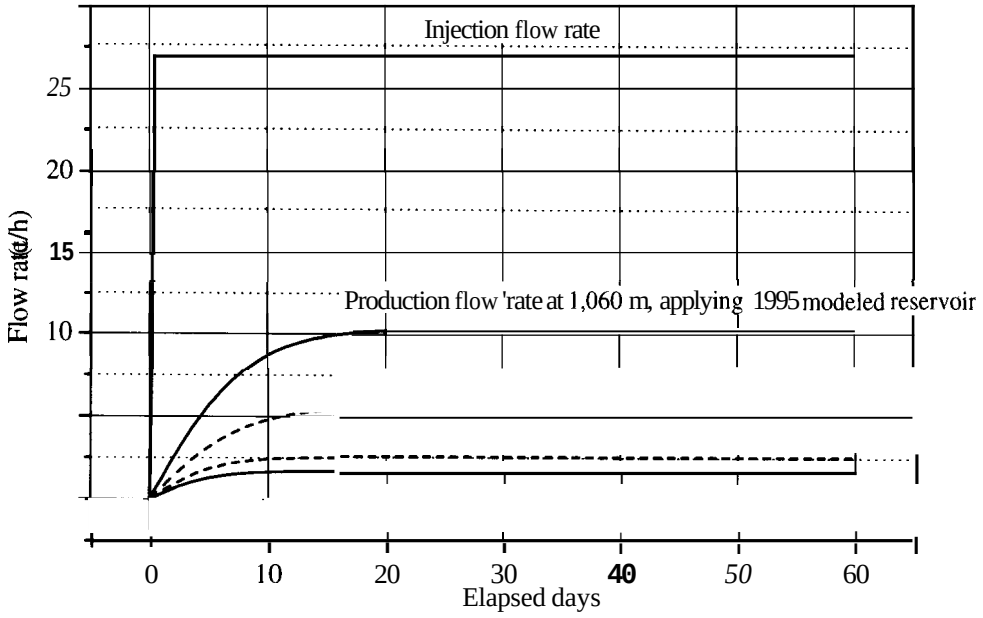

Fig. 10 Predicted production flow rates, comparison between 1994 and 1995 modeled reservoir